Impedance Characteristics of Applied-*B* Ion Diodes

M. P. Desjarlais
Sandia National Laboratories, Albuquerque, New Mexico 87185
(Received 3 August 1987)

A new model of relativistic applied-*B* ion diodes is presented that appears to explain a previously discovered empirical scaling law. The model is based on a self-consistent calculation of the diamagnetic effect on virtual-cathode location coupled with the assumption of a uniform electron-density profile in the sheath. The success of this model greatly increases our understanding of the undesirable phenomenon of impedance collapse in applied-*B* diodes and suggests a simple measure for improving their performance.

PACS numbers: 52.75.Pv, 52.75.Di, 52.80.Vp

Applied-*B* ion diodes[1-3] have been developed for a number of years as a means to produce intense ion beams for application to inertial-confinement fusion (ICF) and have demonstrated many of the requirements for ICF.[4] However, the impedance control of basic applied-*B* diodes has been unsatisfactory and must be improved for ICF applications. A theory is presented that appears to explain the observed impedance characteristics of applied-*B* diodes and suggests a solution to the problem of impedance collapse.

A schematic of such a device appears in Fig. 1. The diode is situated at the end of a magnetically insulated transmission line (MITL) connected to a high-energy pulsed-power accelerator. The diode is symmetric in the azimuthal ($\hat{\theta}$) direction and about the midplane ($z=0$). The aspect ratio R/d is typically much greater than unity; Cartesian coordinates, as shown, are used in the analysis. A sufficiently strong axial magnetic field $\mathbf{B}=B_0\hat{\mathbf{z}}$ is applied to inhibit the flow of electrons across the gap, thereby maximizing the energy delivered to the ion beam. The resulting electron sheath drifts primarily in the $\mathbf{E}\times\mathbf{B}_z$ direction. Although electron losses do occur, such as those resulting from the inevitable symmetry-breaking perturbations,[5] these losses have not been prohibitively high; a number of experiments have achieved ion-current efficiencies (I_i/I_t) on the order of 80% to 90%.[6]

The impedance generally starts out very high. As the electron charge accumulates in the gap, the ion current increases as a result of the space-charge neutralization and the impedance falls.[7] A convenient normalization for the ion current is the single-species Child-Langmuir current. This is the ion current that would flow from a space-charge–limited anode in the absence of electrons and is given in meter-kilogram-second units by

$$I_{CL}=\tfrac{4}{9}\epsilon_0 A(2q/M)^{1/2}V^{3/2}/d^2,$$

where A is the anode emitting area, q/M is the ion charge-to-mass ratio, V is the diode voltage, and d is the anode-cathode gap. The impedance of the diode, under the assumption of $\approx 100\%$ ion-current efficiency, is then simply $Z\approx V/I_i\propto V^{-1/2}(I_i/I_{CL})^{-1}$. A potentially serious limitation of applied-*B* ion diodes has been the fact that experimentally the ion-current enhancement (I_i/I_{CL}) has increased dramatically over the course of the pulse, resulting in a rapidly falling impedance or impedance collapse. It was recently discovered by Miller[8] that data obtained at peak power from applied-*B* diode experiments on the Proto-I, Proto-II, and PBFA-I accelerators demonstrated what appeared to be an empirical relation between the ion-current enhancement and

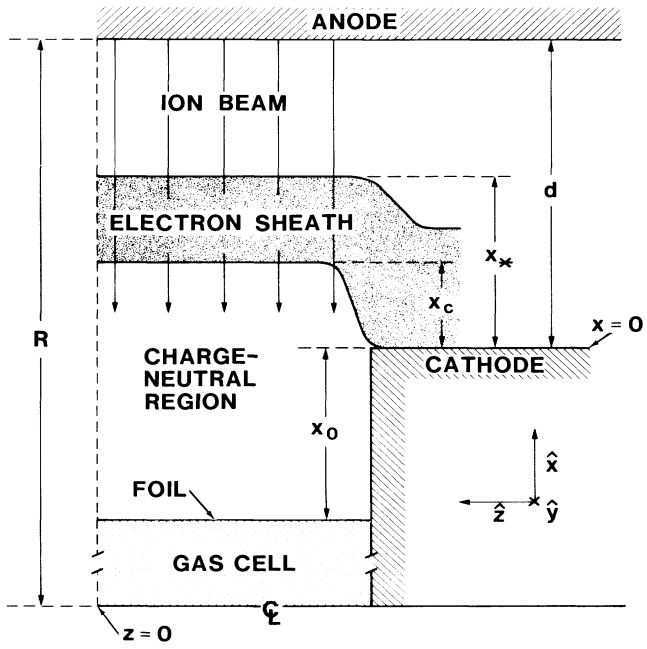

FIG. 1. Applied-*B* diode schematic and coordinate system.

the ratio of the diode self-field $B_\theta = \mu_0 I_t / 4\pi R$ to the critical field for ideal (perfect symmetry) electron insulation B_{cr}. Previous diode models are not successful in explaining applied-B diode impedance characteristics or the empirical scaling discovered by Miller.

The earlier ion-diode models are based on simple geometries and physical assumptions: The anode and cathode are parallel conductors; electrons enter the system with zero total energy H and canonical momentum P_y, and maintain these values over the entire pulse; a uniform magnetic field is applied in the $\hat{\mathbf{z}}$ direction; relativistic and electromagnetic effects are included self-consistently. Within these constraints, two very different equilibria have been proposed. In the Bergeron model,[9] all electrons have the same cycloidlike trajectory with a turning point at the cathode and at the upper sheath surface x_*. In the Antonsen-Ott model,[10] electrons move laminarly along equipotential surfaces at the $\mathbf{E}\times\mathbf{B}_z$ velocity. Neither of these models predicts even moderate ion-current enhancements unless the applied magnetic field is very close to the critical field for ideal insulation, a regime that is not viable experimentally because of high nonideal electron losses. The singular solutions represented by the earlier models are only first approximations in the presence of fluctuations.

A more serious difficulty, encountered in the attempt to apply these models to applied-B diodes, results from the fact that these diodes have generally relied on virtual cathodes as opposed to the rigid conductor assumed in the models. The virtual cathode, defined by $\mathbf{E}=0$, is, to an excellent approximation, coincident with the magnetic-flux surface conformal to the cathode feed surface. This follows from the fact that electrons are born in the feeds with $H=0$ and $P_y=0$, and the virtual-cathode electrons essentially maintain these values. Therefore, since $v_y = (P_y + eA_y)/\gamma m \approx -E_x/B_z$, the $E=0$ surface is tied to the $A_y=0$ flux surface. However, as simulations have demonstrated,[11] out in the diode this surface, x_c, is pushed toward the anode by diamagnetic effects. To describe properly an applied-B diode, it is necessary to calculate the virtual-cathode location self-consistently. Since the virtual cathode is coincident with a well-defined flux surface and the total flux is conserved, the flux between the virtual cathode and the gas-cell foil (see Fig. 1) is known and constant. With the assumption that the azimuthal current in the region $x < x_c$ is negligible, the magnetic field in this region is independent of x. Flux conservation then requires that $B_c(x_0 + x_c) = B_0 x_0$, where B_c is the self-consistent magnetic field at the virtual cathode. This condition, along with a suitable description of the electron distribution for $x \geq x_c$, is sufficient to determine the virtual-cathode location.

To model the electrons in the sheath, I assume that the electron-density profile is flat and that the electrons move laminarly at the velocity $\mathbf{E}\times\mathbf{B}_z$; they are thus unaffected by the self-field of the ion current B_y. The flat density profile is easy to work with and is a more physical approximation in the presence of fluctuations than the earlier sheath models. The constant-density assumption appears *a posteriori* to be a good one.

The equilibrium is naturally divided into three regions: the charge-neutral region $-x_0 \leq x \leq x_c$; the region $x_c \leq x \leq x_*$, where both the sheath electrons and ions are present; and the region $x_* \leq x \leq d$, where only ions are present. Electrons are readily drawn off the side walls and along the magnetic field to neutralize the ion charge in the region $-x_0 \leq x \leq x_c$. In steady state, the electric field in this region is zero and $B_z = B_z(x_c)$. The solution for $x \geq x_c$ is more naturally determined in the variable $\eta = x - x_c$. The virtual-cathode location is given by $\eta = 0$, the sheath surface by $\eta = \eta_*$, and the anode by $\eta = \eta_d$. Within the sheath, the electrostatic potential is described by

$$d^2\bar{\phi}/d\eta^2 = k_e^2 - k_i^2, \tag{1}$$

where $\bar{\phi} = e\phi/mc^2$, $k_e^2 = n_e e^2/\epsilon_0 mc^2$, $k_i^2 = n_i qe/\epsilon_0 mc^2$, m is the electron mass, $-e$ is the electron charge, and q is the ion charge. The boundary conditions are $\bar{\phi}(0)=0$, $\bar{\phi}'(0)=0$, and $\bar{\phi}(\eta_d) = eV/mc^2$. The ions are sufficiently massive to be treated nonrelativistically at the voltages of interest. Their velocity as a function of potential is found through energy conservation: $v(\phi) = [2q(V-\phi)/M]^{1/2}$. In steady state, the ion flux $\Gamma_i = n_i v$ is constant. Therefore $k_i^2(\bar{\phi}) = K^2/(\bar{V}-\bar{\phi})^{1/2}$ where $K^2 = e^2\Gamma_i(qM/em)^{1/2}/\sqrt{2}\epsilon_0 mc^3$ is a constant to be determined.

The vector potential in the sheath is found from

$$d^2\bar{A}_y/d\eta^2 = k_e^2 v_y/c, \tag{2}$$

where $\bar{A}_y = eA_y/mc$. The electrons are assumed to move laminarly at the velocity $\mathbf{E}\times\mathbf{B}_z$; therefore $v_y/c = (d\bar{\phi}/d\eta)(d\bar{A}_y/d\eta)^{-1}$. The boundary conditions on $\bar{A}_y$ are $\bar{A}_y(0)=0$ and $\bar{A}_y(\eta_d) = eB_0 d/mc \equiv \bar{A}_d$. The second condition is simply a result of flux conservation between the cathode and anode.

The equilibrium equations in the sheath region are then

$$d^2\bar{\phi}/d\eta^2 = k_e^2 - K^2/(\bar{V}-\bar{\phi})^{1/2}, \tag{3a}$$

$$\frac{d^2\bar{A}_y}{d\eta^2} = \frac{k_e^2\, d\bar{\phi}/d\eta}{d\bar{A}_y/d\eta}, \tag{3b}$$

whereas in the electron-free region $(x_* < x \leq d)$

$$d^2\bar{\phi}/d\eta^2 = -K^2/(\bar{V}-\bar{\phi})^{1/2}, \tag{4a}$$

$$d^2\bar{A}_y/d\eta^2 = 0. \tag{4b}$$

The integration of these equations and the matching of the potentials and their derivatives at $\eta = \eta_*$, the sheath surface, yields four equations for the four unknowns

η_*/η_d, $k_e\eta_d$, $\bar{\phi}_*$, and $K\eta_d$:

$$k_e\eta_d\frac{\eta_*}{\eta_d}=\frac{1}{\sqrt{2}}\int_0^{\bar{\phi}_*}\frac{d\bar{\phi}}{[(\bar{\phi}-\bar{\phi}_*)+\bar{\phi}_*(1-\bar{\phi}/\bar{V})^{1/2}]^{1/2}}, \tag{5}$$

$$2k_e^2\eta_d^2\bar{\phi}_*=4K^2\eta_d^2\bar{V}^{1/2}, \tag{6}$$

$$2K\eta_d(1-\eta_*/\eta_d)=\tfrac{4}{3}(\bar{V}-\bar{\phi}_*)^{3/4}, \tag{7}$$

$$\bar{A}_d-(2\bar{\phi}_*+\beta)^{1/2}k_e\eta_d(1-\eta_*/\eta_d)=\frac{1}{\sqrt{2}}\int_0^{\bar{\phi}_*}\left[\frac{2\bar{\phi}+\beta}{(\bar{\phi}-\bar{\phi}_*)+\bar{\phi}_*(1-\bar{\phi}/\bar{V})^{1/2}}\right]^{1/2}d\bar{\phi}, \tag{8}$$

where $\beta\equiv\bar{B}_c^2/k_e^2$ and $\bar{B}_c=d\bar{A}_y(0)/d\eta$. Self-consistency and physical considerations put restrictions on the value of the equilibrium constant β; these will be discussed below.

Equations (6)–(8) can be combined to obtain an equation for $\bar{\phi}_*(\bar{V},\bar{A}_d,\beta)$. This is solved numerically. Given $\bar{\phi}_*$, the remaining quantities are easily obtained from combinations of Eqs. (5)–(7). It is clear that the four unknowns are functions of only $\bar{V}$, $\bar{A}_d$, and β. Therefore, if these quantities are fixed, $k_e\eta_d=\text{const}\equiv C_1$ and $K\eta_d=\text{const}\equiv C_2$. Thus, $\bar{B}_c=\beta^{1/2}C_1/\eta_d$. The flux conservation requirement $\bar{B}_c(x_0+x_c)=\bar{B}_0x_0$, along with the definition $\eta_d=d-x_c$, is now used to find x_c:

$$x_c=[(\bar{B}_0d-\beta^{1/2}C_1)/(\bar{B}_0x_0+\beta^{1/2}C_1)]x_0. \tag{9}$$

The ion current is given by $I_i=q\Gamma_iA$, or

$$\frac{I_i}{I_{CL}}=\frac{9}{4}\frac{C_2^2}{\bar{V}^{3/2}}\frac{d^2}{(d-x_c)^2}=\frac{I_i^0}{I_{CL}}\frac{d^2}{(d-x_c)^2}, \tag{10}$$

where I_i^2/I_{CL} is the ion-current enhancement in the limit $x_0\to 0$ ($x_c\to 0$).

To model an applied-B diode at peak power, and thus compare with the data analyzed by Miller, I assume that fluctuations have caused the electron sheath to saturate, $\eta_*\to\eta_d$. This condition fixes β through Eq. (8) with $\bar{\phi}_*=\bar{V}$. The equation

$$\bar{A}_d=\frac{1}{\sqrt{2}}\int_0^{\bar{V}}\left[\frac{2\bar{\phi}+\beta}{(\bar{\phi}-\bar{V})+\bar{V}(1-\bar{\phi}/\bar{V})^{1/2}}\right]^{1/2}d\bar{\phi} \tag{11}$$

must be solved numerically for $\beta=\beta_{sat}$.

Clearly, β_{sat} must be greater than zero for a real solution. However, a further potential restriction must be considered. Analysis of the electron equations of motion reveals that the laminar trajectories are unstable in a thin region near the cathode for $\beta_{sat}<0.5$. In all cases considered in this Letter, the unstable region does not extend to more than 5% of the total diode potential and in most cases is much smaller or not present. Therefore, if the flat-density-profile approximation is still valid, the nonlaminar electron dynamics in this region will not significantly change the solution. It is nevertheless important to bear in mind that the assumptions of this model begin to break down as $\beta\to 0$.

The plot in Fig. 2 is a comparison of the results of this model with the empirical curve found by Miller.[8] The solid curve is Miller's least-squares fit given by $I/I_{CL}=K_1+K_2(B_\theta/B_{cr})^{K_3}$, where $K_1=5.58$, $K_2=6.39$, and $K_3=1.35$. The spread in Miller's data relative to the least-squares fit is very small; however, typical error bars of $\pm 20\%$ on data of this sort are marked on the plot for consideration. The remaining curves give the theoretical results of this model for several of the experiments analyzed by Miller. The uppermost point on each curve corresponds to the experimental voltage at peak power; the solution for lower voltages is given by the dotted curve leading up to this point. The limit $B_\theta\to 0$ is the limit of vanishing ion current, which corresponds to $V\to 0$. The theoretical saturated enhancement is the same for all the experimental configurations in this limit; $I/I_{CL}\to 9\pi^2/16\approx 5.55$ as $V\to 0$. The flat-density-profile assumption, which results in the limiting enhancement of 5.55, is consistent, keeping in mind the limitations of the data, with the 5.58 found by Miller. In each case the theoretical curve is generated with use of the experimental values for d, x_0, and B_0. These values are 3.5 mm, 2.0 mm, and 2.9 T for the 4.5-cm-radius Proto-I diode (triangle); 5.2 mm, 4.8 mm, and 1.65 T for the 14.0-cm-

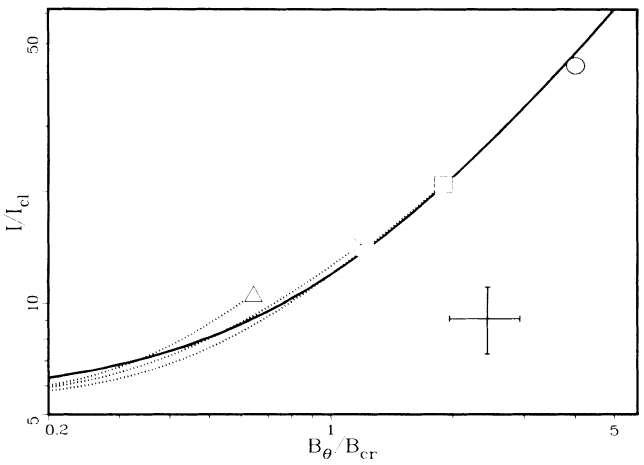

FIG. 2. Comparison of theoretical results (dotted curves) with the empirical scaling (solid curve) of enhancement with total diode current for the Proto-I (triangle), Proto-II (square), and PBFA-I (cross) diodes. The PBFA-I diode with a 16.5% increase in voltage is also shown (circle).

radius Proto-II diode (square); and 5.5 mm, 11.5 mm, and 1.4 T for the 15-cm-radius PBFA-I diode (cross). The circle represents the PBFA-I diode with a further 16.5% increase in the voltage. This value was chosen to match the experimentally determined enhancement. This illustrates the sensitivity of the analytical results to experimental uncertainties at the higher enhancement levels. Very similar behavior results from changes in the level of insulation. Given the experimental uncertainties in the data and the economy of physics in the model, the agreement between the theoretical results and the data analyzed by Miller is very good. Particularly striking is the reproduction of the general trend of I/I_{CL} vs B_θ/B_{cr} found empirically.

Given the model's simple physics and reasonable assumptions, along with the absence of free parameters, it appears that the experimentally observed impedance characteristics of applied-B diodes have a compelling theoretical explanation; the scaling of enhancement with voltage is a basic consequence of the self-consistent diamagnetic effect on virtual-cathode location. The assumption of a flat-density profile at saturation generates excellent agreement with the experimental data obtained at peak power.

The suggested improvement to applied-B diodes is either to reduce x_0 to zero, thus bringing a flux-excluding surface flush with the cathode tips, or, should plasma expansion from the gas cell be a problem, to insert azimuthally symmetric conducting rings or vanes that serve to tie down the virtual-cathode flux surface. From Eq. (9) it follows that the virtual-cathode location is fixed at $x=0$ and the saturated enhancement is limited to 5.55, independent of voltage.

[1]R. N. Sudan and R. V. Lovelace, Phys. Rev. Lett. **31**, 1174 (1973).

[2]P. L. Drieke, C. Eichenberger, S. Humphries, Jr., and R. N. Sudan, J. Appl. Phys. **47**, 85 (1977).

[3]D. J. Johnson, R. J. Leeper, W. A. Stygar, R. S. Coats, T. A. Mehlhorn, J. P. Quintenz, S. A. Slutz, and M. A. Sweeney, J. Appl. Phys. **58**, 12 (1985).

[4]J. P. VanDevender and D. L. Cook, Science **232**, 831 (1986).

[5]M. P. Desjarlais and R. N. Sudan, Phys. Fluids **29**, 1245 (1986), and **30**, 1536 (1987).

[6]D. J. Johnson, P. L. Drieke, S. A. Slutz, R. J. Leeper, E. J. T. Burns, J. R. Freeman, T. A. Mehlhorn, and J. P. Quintenz, J. Appl. Phys. **54**, 2230 (1983).

[7]P. A. Miller and C. W. Mendel, Jr., J. Appl. Phys. **61**, 529 (1987).

[8]P. A. Miller, J. Appl. Phys. **57**, 1473 (1985).

[9]K. D. Bergeron, Phys. Fluids **20**, 688 (1977).

[10]T. M. Antonsen, Jr., and E. Ott, Phys. Fluids **19**, 52 (1976).

[11]S. A. Slutz, D. B. Seidel, and R. S. Coats, J. Appl. Phys. **59**, 11 (1986).